J. Appl. Mech. **84** , (2017) 034501-1 -4

Technical brief: Knockdown factor for the buckling of spherical shells containing large-amplitude geometric defects

Francisco López Jiménez[1], **Joel Marthelot**[1], **Anna Lee**[2], **John W. Hutchinson**[3], **Pedro M. Reis**[1,2]
[1]Department of Civil and Environmental Engineering, Massachusetts Institute of Technology, Cambridge, MA 02139
[2]Department of Mechanical Engineering, Massachusetts Institute of Technology, Cambridge, MA 02139
[3]School of Engineering and Applied Sciences, Harvard University, Cambridge, MA 02138

We explore the effect of precisely defined geometric imperfections on the buckling load of spherical shells under external pressure loading, using finite element analysis that was previously validated through precision experiments. Our numerical simulations focus on the limit of large amplitude defects and reveal a lower bound that depends solely on the shell radius to thickness ratio and the angular width of the defect. It is shown that, in the large amplitude limit, the buckling load depends on an single geometric parameter, even for shells of moderate radius to thickness ratio. Moreover, numerical results on the knockdown factor are fitted to an empirical, albeit general, functional form that may be used as robust design guideline for the critical buckling conditions of pressurized spherical shells.

1 Introduction

Since the beginning of the 20th century it has been observed that experimental studies on the buckling of thin shells can result in maximum loads as low as 20% of the classical theoretical predictions [1]. The ratio between the experimentally observed and theoretically predicted values of the critical buckling pressure is known as the *knockdown factor*. Early efforts to come to terms with this discrepancy between experiments and shell theory focused on the post-buckling behavior of imperfect shells [2,3] and their extreme sensitivity to initial imperfections [4]. Following extensive studies involving a variety of shell structures, loading conditions and imperfections [5–9], it became well established that the primary cause for this *knockdown factor* is the presence of geometric imperfections [10]. Nonetheless, despite significant theoretical and computational efforts in understanding imperfection sensitivity, practical designs of curved shells have traditionally made use of empirical knockdown factors [11,12]. In contrast to this approach, efforts currently underway by NASA and others in the aerospace industry aim at developing deterministic design guidelines based on manufacturing-specific imperfection distribution [13–15].

Leveraging a novel rapid prototyping technique to fabricate elastomeric spherical shells with nearly uniform thickness [16], we have recently investigated [17] the critical buckling conditions of spherical shells containing precisely engineered geometric imperfections. By means of experiments, simulations and theory, our results showed that the experimental buckling pressures can be accurately predicted, as long as the exact geometry of the imperfection is appropriately included in theoretical construct [17,18]. Moreover, for large imperfections, we found a critical buckling pressure can become independent of the amplitude of the defect, such that the knockdown factor exhibits a robust plateau. Note that an earlier study [19] had provided numerical evidence for the existence of this plateau, but a systematic characterization had not been done until our more recent investigation [17]. These findings provide further evidence that replacing the current empirical knowndown guidelines [12] by a deterministic framework may be within reach.

In this Technical Brief, we augment our previous analysis [17] to provide a quantitative characterization of the lower bounds of the critical buckling pressure of large-amplitude, dimple-like geometric defects, which we show depend on a combination of shell radius to thickness ratio and angular width of the defect. Whereas previously we focused on a combination of experiments, reduced shell theory and simulations, here, we focus on gaining further insight from the previously validated finite element analysis.

2 Methodology: Finite Element Analysis

The simulations were performed using the commercial FEM package Abaqus/Standard. The shells are hemispheres clamped at the equator. We use axisymmetry to reduce the computational cost, since it has been shown that non-axisymmetric bifurcations only take place far into the post-buckling regime [18]. The material was treated as an incompressible Neo-Hookean solid, with reduced hybrid axisymmetric elements CAX4RH. The loading was modeled as live pressure on the outer surface of the structure. Given the unstable postbuckling behavior of the shells, the simulations

used the Riks method [20], which simultaneously solves for loads and displacements, measuring the progress of the simulation with the arc-length of the load-displacement curve.

The buckling pressure was defined as the maximum pressure, p_{max}, attained during the analysis, and the *knockdown factor* is defined as $\kappa_d = p_{max}/p_c$. Here, p_c is the classic theoretical buckling load for a spherical shell under uniform external pressure, obtained from a linear buckling analysis [21]:

$$p_c = \frac{2E}{\sqrt{3(1-\nu^2)}}\eta^{-2}, \tag{1}$$

where E is Young's modulus, ν is Poisson's ratio, and $\eta = R/t$ is the dimensionless radius of the shell, of radius R and thickness t. The radius and thickness of our shells have been varied systematically to explore the range $50 < \eta < 1000$. The mesh density was varied with η to keep a regular aspect ratio for the elements, while maintaining a sufficiently fine mesh through the thickness. The discretization in the radial direction involved between 6 and 20 elements, and between 1000 and 5000 in the angular direction.

The initial geometric imperfections were directly introduced in the mesh as a normal displacement of the middle surface, with the profile of a Gaussian dimple:

$$w_I = -\delta e^{-(\beta/\beta_0)^2}, \tag{2}$$

where β is the angular measure from the pole, and δ and β_0 are parameters that control the depth and angular width of the defect, respectively. The rest of the mesh is then defined assuming constant thickness t perpendicular to the middle surface. For the remainder of this article, we normalize the amplitude of the defect by the thickness of the shell, $\bar{\delta} = \delta/t$.

Finally, following the work of Koga and Hoff [22], we introduce the geometric parameter:

$$\lambda = \left\{12(1-\nu^2)\right\}^{1/4}\eta^{1/2}\beta_0, \tag{3}$$

which combines the radius to thickness ratio of the shell, η, and the angular width of the imperfection, β_0, in a single parameter. It should be noted that this parameter is often used in the literature to describe the geometry of shallow spherical shells, in which case it is defined using the edge-angle of the complete shell [23–26]. Our previous results [17] indicated that λ is an appropriate and effective single geometric parameter to characterize how the defect dictates the imperfection sensitivity of our imperfect shells.

3 Results

We start our investigation by further substantiating the appropriateness of using the parameter λ defined in Eq. (3) to characterize the effect of dimple-like defects. In Fig. 1a, we plot a contour map of the knockdown factor κ_d, for a constant normalized defect amplitude $\bar{\delta} = 1$ and different values of the dimensionless radius, η, and the angular width of the defect, β_0. The data show contour lines of constant κ_d align with lines of constant λ (solid, dashed and dashed-dot red lines). In particular, $\lambda = 2.625$ is the critical geometric parameter for the chosen defect amplitude, $\bar{\delta} = 1$: it describes the combination of η and β_0 for which a defect of the same amplitude as the shell thickness results in the largest reduction of critical buckling load. A departure between our numerical results and a description that depends only on λ is only observed when $\lambda > 10$, for which the influence of the defect on the buckling pressure is too small to be captured accurately by our simulations.

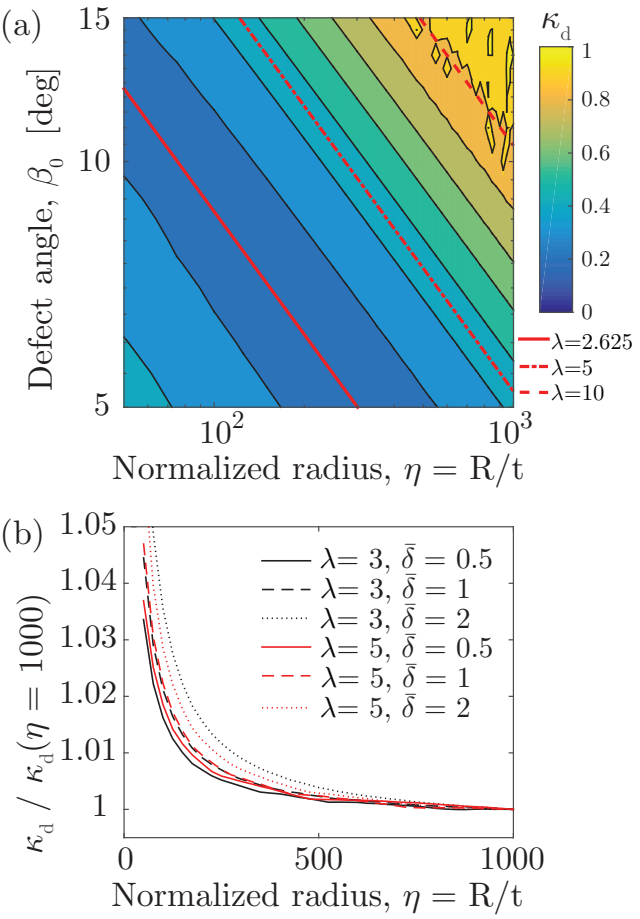

Fig. 1. (a) Contour plot of the knockdown factor, κ_d, for different values of the normalized radius, η, and defect angle, β_0. The solid, dashed and dashed-dot red lines correspond to instances of constant geometric parameter λ (see legend). (b) Knockdown factor, κ_d, versus normalized radius, η, normalized by $\kappa_d(\eta = 1000)$, for different values of λ and $\bar{\delta}$.

In order to further investigate how the knockdown factor depends on the value of the radius to thickness ratio, in Fig. 1b, we plot κ_d versus η, for different values of λ and $\bar{\delta}$. Each curve is normalized by the value corresponding to the

closest case to the thin shell limit considered in this study ($\eta = 1000$). As expected, the results show a clear convergence as η increases. Even for $R/t = 100$, the deviations between curves with different values of λ and $\bar{\delta}$ are at most 5%. It is important to note that the chosen combinations of $\bar{\delta}$ and λ correspond to values of the knockdown factor spanning the range $0.2 < \kappa_d < 0.7$, further emphasizing the generality of the results.

As it was also shown in our previous study [17], for a given choice of λ, κ_d decreases as the amplitude of the defect $\bar{\delta}$ increases. Importantly, past a critical defect amplitude, $\bar{\delta}_{plateau}$, the curve reaches a plateau; once the defects are sufficiently large, the buckling pressure of the shell does not depend on the magnitude of the defects. In the inset of Fig. 2, we plot a typical example of such behavior, for $\eta = 100$ and $\lambda = 2.5$. We now turn to study the knockdown factor in the plateau regime, $\langle \kappa_d \rangle_{plateau}$, which in this case is defined as the value of the curve in which $|d\kappa_d/d\bar{\delta}| \leq 0.025$. Using different values for this threshold (e.g., 0.005, 0.01 or 0.05) has a negligible effect on the results.

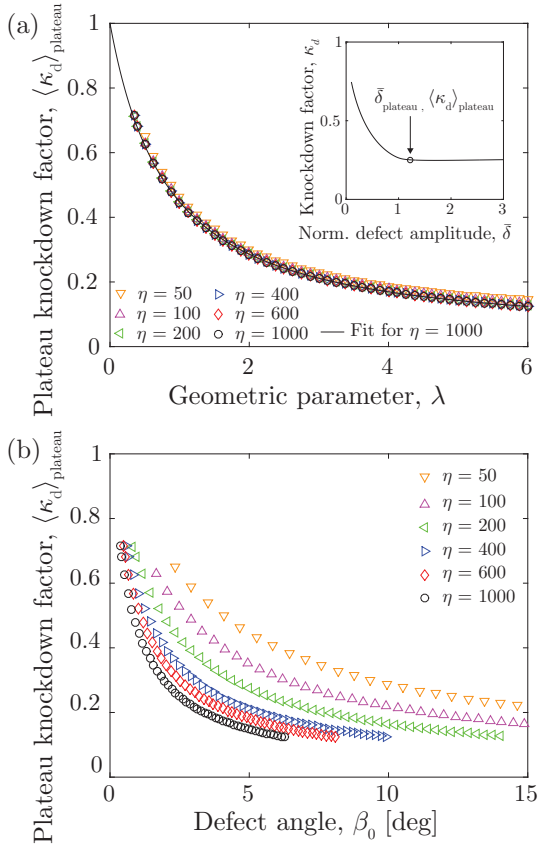

Fig. 2. (a) Plateau knockdown factor, $\langle \kappa_d \rangle_{plateau}$, as a function of the geometric parameter, λ, for different values of the dimensionless radius, η. The solid line corresponds to the fit of the data to Eq. 4, using the numerical values for $\eta = 1000$. Inset: representative example of κ_d versus $\bar{\delta}$, for $\lambda = 2.5$ and $\eta = 100$. (b) Plateau knockdown factor, $\langle \kappa_d \rangle_{plateau}$, as a function of the defect angle, β_0, for different values of the dimensionless radius, η.

In Fig. 2a we plot $\langle \kappa_d \rangle_{plateau}$ as a function of the geometric parameter λ, for different values of η. As it was the case in Fig. 1b, the deviations as a function of η are small, especially for $\lambda > 2$. The values of $\langle \kappa_d \rangle_{plateau}$ decay as λ increases, which corresponds physically to either shells of decreasing η, or increasing defect width. It should be pointed out that for $\eta \geq 100$ it was not possible to scan the whole range $0.35 < \lambda < 6$, as with the other shells, since our definition of the deformed geometry, Eq. 2, resulted in self-contact of the shells for such narrow defects.

The numerical results plotted in Fig. 2a have been used to fit an empirical function of the form:

$$\langle \kappa_d \rangle_{plateau} = \frac{1-b}{(1+\lambda)^a} + b \tag{4}$$

which fulfills the condition of $\langle \kappa_d \rangle_{plateau} = 1$ for defects of negligible width (in the limit of $\lambda \to 0$) and allows for a constant value for large values of λ. In Fig. 2a, we superpose the fit (solid line) to the data, for the specific case of $\eta = 1000$. The corresponding values of the fitting parameters (b and a), are shown in Table 1 (along with those for other cases of η). The results are very similar for different values of the radius to thickness ratio, with a clear convergence to the thin shell limit once $\eta \geq 200$. In fact, the fitting parameters $\bar{a} = -1.23 \pm 0.01$ and $\bar{b} = 0.036 \pm 0.003$, obtained using the complete set of data, provide an approximation with at most 11% of error in the case of $\eta = 50$, and less than 5% for all other values of η.

η	a	b
50	-1.20 ± 0.02	0.050 ± 0.005
100	-1.24 ± 0.01	0.048 ± 0.002
200	-1.23 ± 0.01	0.040 ± 0.003
400	-1.23 ± 0.01	0.038 ± 0.003
600	-1.23 ± 0.01	0.037 ± 0.003
1000	-1.23 ± 0.01	0.036 ± 0.003
All	-1.23 ± 0.01	0.041 ± 0.003

Table 1. Results for the fit of Eq.4 using numerical results with different values of the normalized radius, η, in the range $0.35 < \lambda < 6$. The $\pm$ uncertainty correspond to the 95% confidence interval obtained by fitting the data.

In order to provide a more physical interpretation of our data, in Fig. 2b we plot the same values of $\langle \kappa_d \rangle_{plateau}$ shown in Fig. 2a, but now as a function of the angular width of the defect, β_0. These data can be used to estimate a lower bound for the knockdown factor of a spherical shell of known η, as a function of the expected angular width of the defects (i.e., area), and independently of their amplitude (i.e., depth). The

results show that the knockdown factor decreases sharply with the angular width of the defect, specially for very thin shells ($\eta \geq 400$), for which $\langle \kappa_d \rangle_{\text{plateau}} < 0.2$ for defects as small as $\beta_0 > 5^\circ$.

4 Discussions and Conclusions

We have made use of a previously validated finite element analysis [17] to study the buckling of hemispherical shells, and extended our previous numerical exploration to focus on the limit of large-amplitude defects. Note that a recent study [18] found that the critical buckling conditions for hemispherical shell were indistinguishable from the full spherical case, such that our results, here, can be regarded as representative of spherical shells. First, we provided significant evidence that the geometric parameter λ provides a compact quantitative description of the effect of geometric imperfections, even in shells of moderate radius to thickness ratio (e.g. $50 < \eta < 100$). Moreover, we presented a parametric study of the knockdown factor in the plateau regime, $\langle \kappa_d \rangle_{\text{plateau}}$, reached after the amplitude of the defect reaches a critical value, $\bar{\delta}_{\text{plateau}}$.

Note that, in some cases (relatively thicker shells, *e.g.* $\eta < 200$, with large values of the geometric parameter, *e.g.* $\lambda = 5$) the defect may be large enough for the spherical geometry of the shell to be questionable. However, for increasingly thinner shells (*e.g.*, $\eta > 200$) the plateau behavior described throughout this paper is still applicable for these shells that are much closer to the ideal spherical geometry (*i.e.*, small defects). As such, our description of the plateau does appear to be general and intrinsic to the buckling of spherical shells containing geometric imperfections.

Our results, combined with information regarding the expected width of the defects in a given spherical shell, can be used to provide a lower bound for the knockdown factor, independently of the defect amplitude. This is in contrast with the traditional approach, in which design is based on empirical knockdown factors, obtained from experiments on a wide range of shells. We hope that this deterministic design guideline will provide further motivation to the recent resurgence of interest on the buckling of thin shells. In particular, to further establish the generality of the present results, it will be important to systematically consider other shapes of the initial geometric imperfection, including, but not limited to, non-axisymmetric defects.

Acknowledgment

This work was supported by the National Science Foundation (CAREER CMMI-1351449).

References

[1] Elishakoff, I., 2014. *Resolution of the Twentieth Century Conundrum in Elastic Stability*. World Scientific.

[2] von Kármán, T., and Tsien, H.-S., 1939. "The buckling of spherical shells by external pressure". *J. Aeronaut. Sci.,* **7**(2), pp. 43–50.

[3] Tsien, H.-S., 1942. "A theory for the buckling of thin shells". *J. Aeronaut. Sci.*, pp. 373–384.

[4] Koiter, W. T., 1945. "Over de stabiliteit van het elastisch evenwicht". PhD thesis, TU Delft, Delft University of Technology.

[5] Bijlaard, P. P., and Gallagher, R. H., 1960. "Elastic instability of a cylindrical shell under arbitrary circumferential variation of axial stress". *J. Aerospace Sci.*, pp. 854–859.

[6] Kobayashi, S., 1968. "The influence of the boundary conditions on the buckling load of cylindrical shells under axial compression". *J. Japan Society of Aeronautical Engineering,* **16**(170), pp. 74–82.

[7] Almroth, B. O., 1966. "Influence of edge conditions on the stability of axially compressed cylindrical shells". *AIAA J.,* **4**(1), pp. 134–140.

[8] Hutchinson, J. W., and Koiter, W. T., 1970. "Postbuckling theory". *ASME Appl. Mech. Rev.,* **23**(12), pp. 1353–1366.

[9] Budiansky, B., and Hutchinson, J. W., 1972. "Buckling of circular cylindrical shells under axial compression". In *Contributions to the Theory of Aircraft Structures*. Delft University Press, pp. 239–259.

[10] Babcock, C. D., 1983. "Shell stability". *ASME J. Appl. Mech.,* **50**(4b), pp. 935–940.

[11] Seide, P., Weingarten, V., and Peterson, J. P., 1968. "Buckling of thin-walled circular cylinders". *NASA SP-8007*.

[12] Samuelson, L. Å., and Eggwertz, S., 1992. *Shell Stability Handbook*. Elsevier Applied Science, London and New York.

[13] Hilburger, M. W., Nemeth, M. P., and Starnes, J. H., 2006. "Shell buckling design criteria based on manufacturing imperfection signatures". *AIAA journal,* **44**(3), pp. 654–663.

[14] Hilburger, M. W., 2012. "Developing the next generation shell buckling design factors and technologies". In 53rd AIAA/ASME/ASCE/AHS/ASC Structures, Structural Dynamics and Materials Conference.

[15] Castro, S. G. P., Zimmermann, R., Arbelo, M. A., Khakimova, R., Hilburger, M. W., and Degenhardt, R., 2014. "Geometric imperfections and lower-bound methods used to calculate knock-down factors for axially compressed composite cylindrical shells". *Thin. Wall. Struct.,* **74**, pp. 118–132.

[16] Lee, A., Brun, P.-T., Marthelot, J., Balestra, G., Gallaire, F., and Reis, P. M., 2016. "Fabrication of slender elastic shells by the coating of curved surfaces". *Nat. Commun.,* **7**, p. 11155.

[17] Lee, A., López Jiménez, F., Marthelot, J., Hutchinson, J. W., and Reis, P. M., 2016. "The geometric role of precisely engineered imperfections on the critical buckling load of spherical elastic shells". *ASME J. Appl. Mech.,* **83**(11), p. 111005.

[18] Hutchinson, J., 2016. "Buckling of spherical shells revisited". *Proc. R. Soc. A,* **472**(2195), p. 20160577.

[19] Starlinger, A., Rammerstorfer, F. G., and Auli, W., 1988. "Buckling and postbuckling behavior of thin ribbed and unribbed spherical shells under external pressure(beulen und nachbeulverhalten von duennen verrippten und unverrippten kugelschalen unter aussendruck)". *Z. Angew. Math. Mech.,* **68**(4).

[20] Riks, E., 1979. "An incremental approach to the solution of snapping and buckling problems". *Int. J. Solids Struct.,* **15**(7), pp. 529–551.

[21] Zoelly, R., 1915. "Ueber ein knickungsproblem an der kugelschale". PhD thesis, Techn. Wiss. ETH Zürich.

[22] Koga, T., and Hoff, N. J., 1969. "The axisymmetric buckling of initially imperfect complete spherical shells". *Int. J. Solids Struct.,* **5**(7), pp. 679–697.

[23] Kaplan, A., and Fung, Y. C., 1954. A nonlinear theory of bending and buckling of thin elastic shallow spherical shells.

Tech. rep., NACA Technical Note 3212.

[24] Homewood, R. H., Brine, A. C., and Johnson Jr, A. E., 1961. "Experimental investigation of the buckling instability of monocoque shells". *Exp. Mech.,* **1**(3), pp. 88–96.

[25] Seaman, L., 1962. "The nature of buckling in thin spherical shells". PhD thesis, Massachusetts Institute of Technology.

[26] Krenzke, M. A., and Kiernan, T. J., 1963. "Elastic stability of near-perfect shallow spherical shells". *AIAA J.,* **1**(12), pp. 2855–2857.